Медицинская иммунология
2022, Т. 24, № 4,
стр. 729-740
© 2022, СПб РО РААКИ

Оригинальные статьи
Original articles

Medical Immunology (Russia)/
Meditsinskaya Immunologiya
2022, Vol. 24, № 4, pp. 729-740
© 2022, SPb RAACI

ИДЕНТИФИКАЦИЯ МУТАЦИЙ ПОВЕРХНОСТНОГО ГЛИКОПРОТЕИНА SARS-CoV-2 В ШТАММАХ, ИЗОЛИРОВАННЫХ В ИРАКЕ

Давуд Али А.[1], Ясим Б.И. [2], Рияд-аль-Джалили О.[1]

[1] *Мосульсий университет, г. Мосул, Ирак*
[2] *Ниневийский университет, г. Мосул, Ирак*

Резюме. Глобальная пандемия коронавирусной инфекции стала длительной кризисной ситуацией для общества, экономики и здравоохранения, которая продолжается и сейчас. Спайк-гликопротеин вируса SARS-CoV-2 является одним из первичных компонентов вирулентности, тканевого тропизма и объектов носительства. Целью работы было определение мутаций S-белка в изолятах от больных COVID-19 в Ираке. Методы: полногеномные последовательности линий вируса в Ираке получали из базы GISAID. Используя статистики сатурационного мутагенеза и другие методики биинформатики, мы изучили 20 последовательностей изолятов SARS-CoV-2 с миссенс-мутацией данного белка, выявленных в Ираке и выбранных из базы данных NCBI. Результаты: во всех линиях вируса, при сравнении с диким типом, были выявлены следующие мутации: L452R, A522V, E583D and D614G. Число мутаций этих линий было различным, в зависимости от места сбора образцов. Мутация D614G была обнаружена в 19 линиях. Одна из линий имела 3 мутации, тогда как другая относились к дикому типу вируса. Структура мутантного белка существенно изменяется из-за энергетических взаимодействий атомов в зоне стыковки, что влияет на стабильность белка. Выводы: стабильность S-белка может изменяться в зависимости от места мутации. Стыковка молекулы RBD-ACE2 нарушается по-разному при заменах аминокислот L452R and A522V.

Ключевые слова: SARS-CoV-2, спайк-протеин, мутации, поверхностные, ACE2, RBD

IDENTIFICATION OF SURFACE GLYCOPROTEIN MUTATIONS OF SARS-CoV-2 IN ISOLATED STRAINS FROM IRAQ

Ali Adel Dawood[a], Bassam Ismael Jasim[b], Omar Riadh Al-Jalily[a]

[a] *University of Mosul, Mosul, Iraq*
[b] *Ninevah University, Mosul, Iraq*

Abstract. Background: The global pandemic of coronavirus disease is a societal, economic, and public-health crisis that is still underway. The spike glycoprotein of SARS-CoV-2 is one of the primary ingredients for virulence, tissue tropism, and host areas. Aim: This study aimed to determine mutations in the S protein of the Iraqi COVID-19 isolates.

Full genome sequences of Iraqi strains were obtained from GISAID. Using statistical saturation mutagenesis and other informatics methods, we investigated 20 sequences of SARS-CoV-2 S protein missense mutation isolates in Iraq selected from NCBI.

Адрес для переписки:
Али А. Давуд
Медицинский колледж Мосульского университета
Аль-Джамеа, 1, г. Мосул, Ирак.
Тел.: 00964 (770)-176-8002.
E-mail: aad@uomosul.edu.iq

Address for correspondence:
Ali A. Dawood
College of Medicine, University of Mosul
Al-Jameaa, st. 1, Mosul, Iraq.
Phone: 00964 (770)-176-8002.
E-mail: aad@uomosul.edu.iq

Образец цитирования:
Али А. Давуд , Б.Р. Ясим, О. Рияд-аль-Джалили «Идентификация мутаций поверхностного гликопротеина SARS-CoV-2 в штаммах, изолированных в Ираке» // Медицинская иммунология, 2022. Т. 24, № 4. С. 729-740. doi: 10.15789/1563-0625-IOS-2455

For citation:
Ali Adel Dawood, Bassam Ismael Jasim, Omar Riadh Al-Jalily "Identification of Surface Glycoprotein Mutations of SARS-CoV-2 in Isolated Strains from Iraq", Medical Immunology (Russia)/Meditsinskaya Immunologiya, 2022, Vol. 24, no. 4, pp. 729-740. doi: 10.15789/1563-0625-IOS-2455

DOI: 10.15789/1563-0625-IOS-2455

The following mutations were detected for all the strains under study compared to the wild type: L452R, A522V, E583D and D614G. The number of mutations in the strains was different depending on the location of the state from which the sample was collected The D614G mutation was found in 19 strains. One strain had three mutations, while the other was a wild form strain. The structure of the mutant protein changes dramatically, as does the energy of the atoms concerning the docking position, affecting the protein's stability.

The mutation sites would improve the S protein's stability. Molecular docking of RBD-ACE2 is affected differently by residues L452R and A522V.

Keywords: SARS-CoV-2, Spike, Mutation, Surface, ACE2, RBD

Introduction

The global pandemic of coronavirus disease is an ongoing social, economic, and public health issue. COVID-19 etiologic agent was recently designated SARS-CoV-2 by the Coronavirus Study Group on the International Committee of Virus Taxonomy [6, 16]. The latest member of the coronaviridae family is closely linked to serious acute coronavirus syndrome [5, 28].

The spike glycoprotein of SARS-CoV-2 is one of the primary ingredients for virulence, tissue tropism, and host areas and plays a key goal for the neutralization of antibodies and the design ofa vaccine [8, 12, 26, 38]. The S protein of SARS-CoV-2 is generally regarded as the most promising immunogenic for eliciting defensive immunity [24]. However, since the S protein has adapted to conduct its functions when evading host neutralizing antibody responses, it should be designed toensure the best immune response possible [13]. The protein of coronavirus S is split into two domains: S1 and S2 [7, 24]. The domain S1 mediates receptor binding and the domain S2 mediates membrane fusion downstream. In S1 there is a core and receptor binding motif (RBM) that explicitly recognizes ACE2 in the recipient binding domain (RBD) [4, 25]. For the host and cross-species SARS-CoV-2 infections, the RBD-ACE2 interactions are important [1, 3]. The recent experiments have shown that the ACE2 affinity of SARS-Cov-2 S protein and bat coronavirus is greater than that of SARS-CoV [16]. The cryogenic electron microscopy (cryo-EM) work has been used to establish a prefusion ectodomain trimer in open and closed SARS-COV-2 S conformation states [34, 35]. The computer modeling of the SARS-CoV-2 RBD-ACE2 interaction has found several residues potentially involved in the interaction, although the true residues which mediate the interaction remain unclear [14, 30]. In addition, no isolated SARS- CoV monoclonal antibodies can neutralize SARS-CoV-2 in place of observable SARS-CoV-2 neutralizing serum/plasma activity in patients recovering from the SARS-CoV infections [19, 23].

Compared to other RNA viruses, coronaviruses are at high rates of mutation. New mutations are constantly emerging in SARS-CoV-2 and are the main challenge in the synthesis of wide neutralizing antibodies [17]. Computational mutagenesis for saturation offers a quick technique for investigating all conceivable mutations and identifying new functional locations. Therefore, it is essential to study RBD-CE2 affinity and S stability.

In this study, the SARS-CoV-2 S missense mutations were investigated with computational saturation mutagenesis. We retrieved 20 completed Iraqi SARS-CoV-2 isolates from various regions. A total of four S-protein mutations and one RBD domain mutation were observed. The future target locations for antiviral drug formulation and vaccines for the latest coronavirus strain study have been identified.

Materials and methods

The current research has conducted complete genome sequence data from the ancestral cladding of SARS-CoV-2 strains presented in GISAID of Iraq viral isolated from Samawa and Erbil (https://www.gisaid.org). NCBI Genbank has been retrieved full genome sequences of 20 SARS- CoV-2 isolates corresponding to the following accession numbers: MW290973, MW512847, MW633517, MW546610, MT940504, MT940484, MT940500, MT940492, MT940489, MT940508, MT940497, MT940487, MT940499, MT940486, MT940496, MT940507, MT940494, MT940503, MT940490, and MT940498. The surface glycoprotein sequences were derived from each genome annotation or by locally aligning the SARS-CoV-2 protein in the coding segment (CDS) translation characteristic: QPI19598, QQW45569, QRW43499, QQZ48538, QNL36298, QNL36058, QNL36250, QNL36154, QNL36118, QNL36346, QNL36214, QNL36094, QNL36238, QNL36082, QNL36202, QNL36334, QNL36226, QNL36178, QNL36286, and QNL36130 (https://www.ncbi.nlm.nih.gov). China-reference entire genome (YP_009724390) and S protein (QQZ48538) were selected as template sequences for alignment and homology modeling.

Multiple sequence alignment and phylogenetic tree analysis

MAFFT 7 server and Clustal-Omega were used for the degree of convergence between sequences. Similarity estimation with Jalview was seen. The phylogenetic tree has been derived with ViPR tool.

Predication of 2D structure

A PSIPRED webserver was used to identify the secondary structural portion (random spool, alpha helices beta-strands) of S protein. Imaging and

comparison of protein structure with PyMoL software were conducted.

Predication of homology modeling and 3D structural analysis

The wild and mutant S protein crystal model was created by homology modeling approach using servers from Swiss-Model and Maestro-Schrodinger. PDB (6VXX) reference of S protein has been selected as a template. Models are built based on the target-template alignment using ProMod3. In the structural validation and model accuracy (protein preparation, covalent geometry, angles of torque, protein minimization, residues scanning estimation, energy calculation, hydrogen bond optimization, and whole atomic contact analysis), BioLuminate 4.2 and QMEAN were used to calculate wild and mutant of S proteins. Images were viewed using PyMol.

The ProtParam in the ExPASy portal has calculated the physiochemical characteristics of wild and mutant S proteins. Inelastic network models, changes caused by mutations in the protein dynamic structure were simulated. The DynOmics 1.0 server is used to analyze S protein structure mutations and complex molecule modifications. By comparing experimentally crystallographic results with wild and mutant model data obtained in this analysis, both the Gaussian network and anisotropic network model measured the collective protein motion and mean quadrangular fluctuations of each residue.

Construction 3D structure of S protein mutations on the molecular docking model

We used Schrodinger sever to build the crystal structure of the detected mutations on the molecular docking region between receptor-binding domain (RBD) and angiotensin-converting enzyme 2 (ACE2) on the host cell membrane. PyMol was used to decipher the images. The RBD-ACE2 model with ID (6M0J) was chosen from the PDB. The distances between the atoms were measured to see whether the mutations influenced the chain of molecular docking or the overall model's conformational changes.

Results

Multiple sequence alignment of 20 S proteins compared with the wild type is shown in Figure (1). Only 1 out of 20 sequences did not notice any changes and adopt the wild form. A total of 4 existing mutations were detected. S gene mutation analysis determined: D614G mutation [aspartic acid (D) substituted with glycine (G) in codon 614]. This mutation is linked to the facilitation of virus transmission and virulence in 19 sequences. Other mutations showed in the S gene

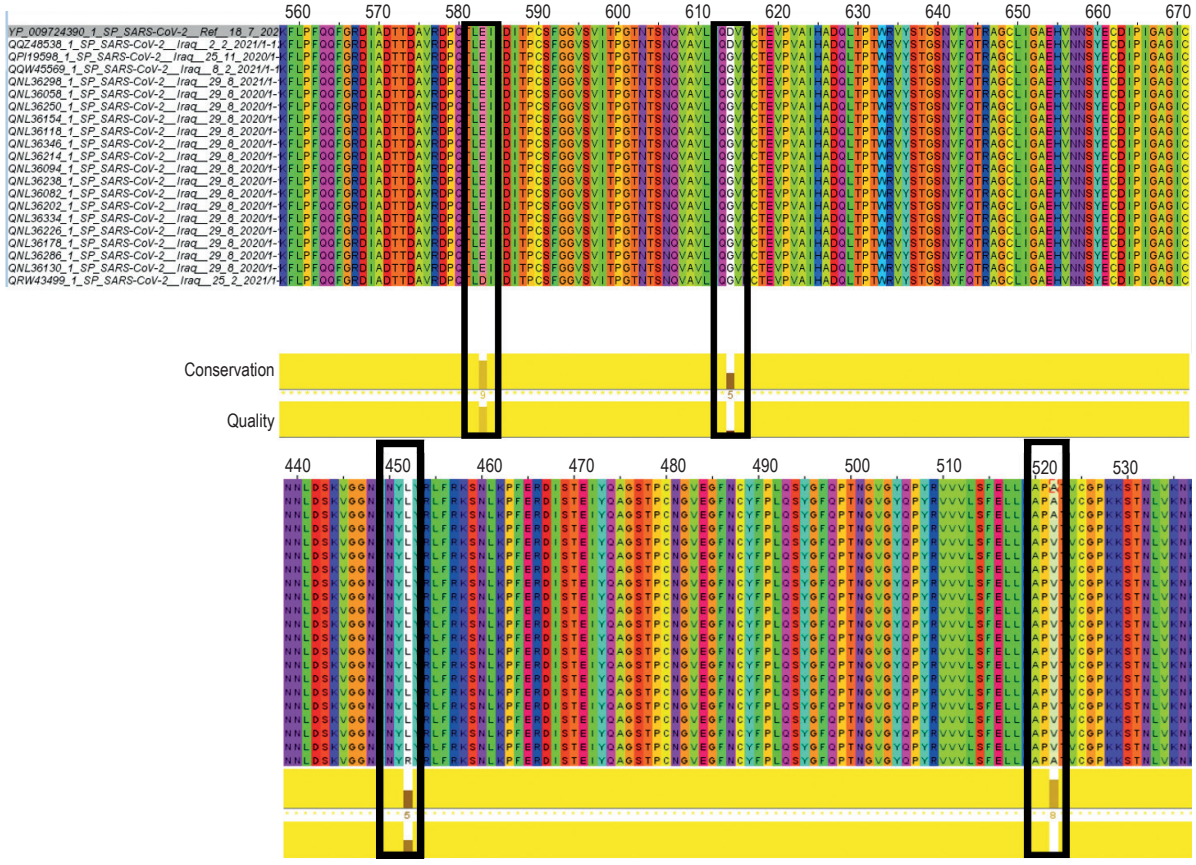

Figure 1. MSA showed 4 mutations in different residues of 19 sequences of S proteins

Note. Mutations are L452R, A522V, E583D and D614G. Each strain shows the numbers of mutations. D614G is found in 19 starins.

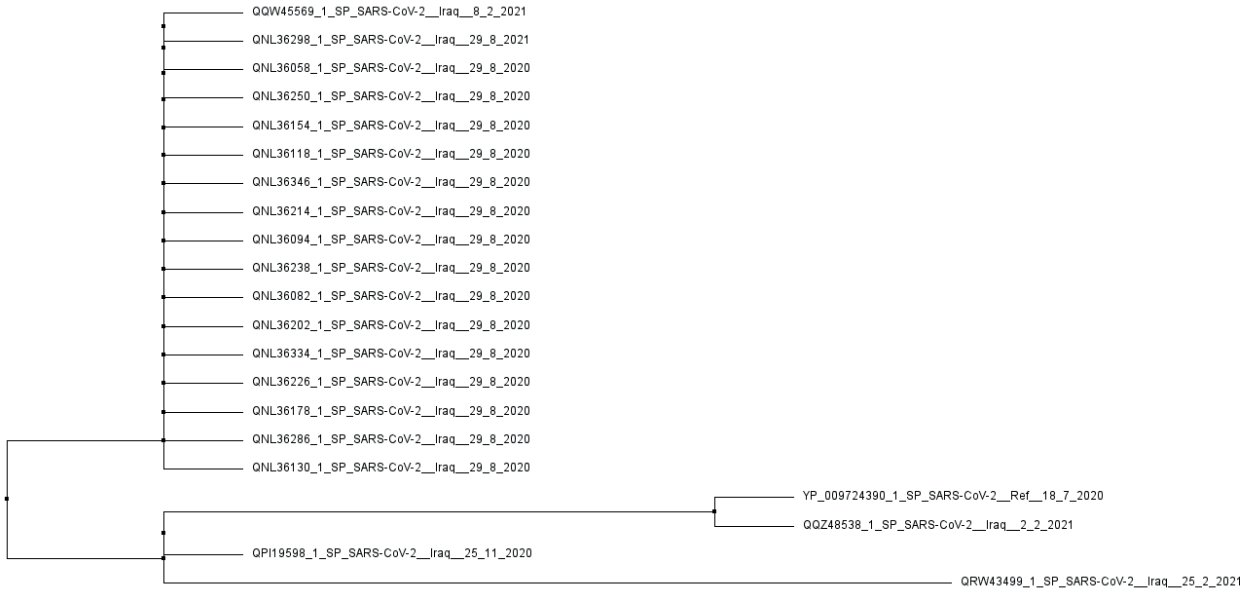

Figure 2. Phylogenetic tree of 21 sequences of S protein

Note. The QNL36238 strain is related to the wild type. 17 strains are not closely related to the wild strain.

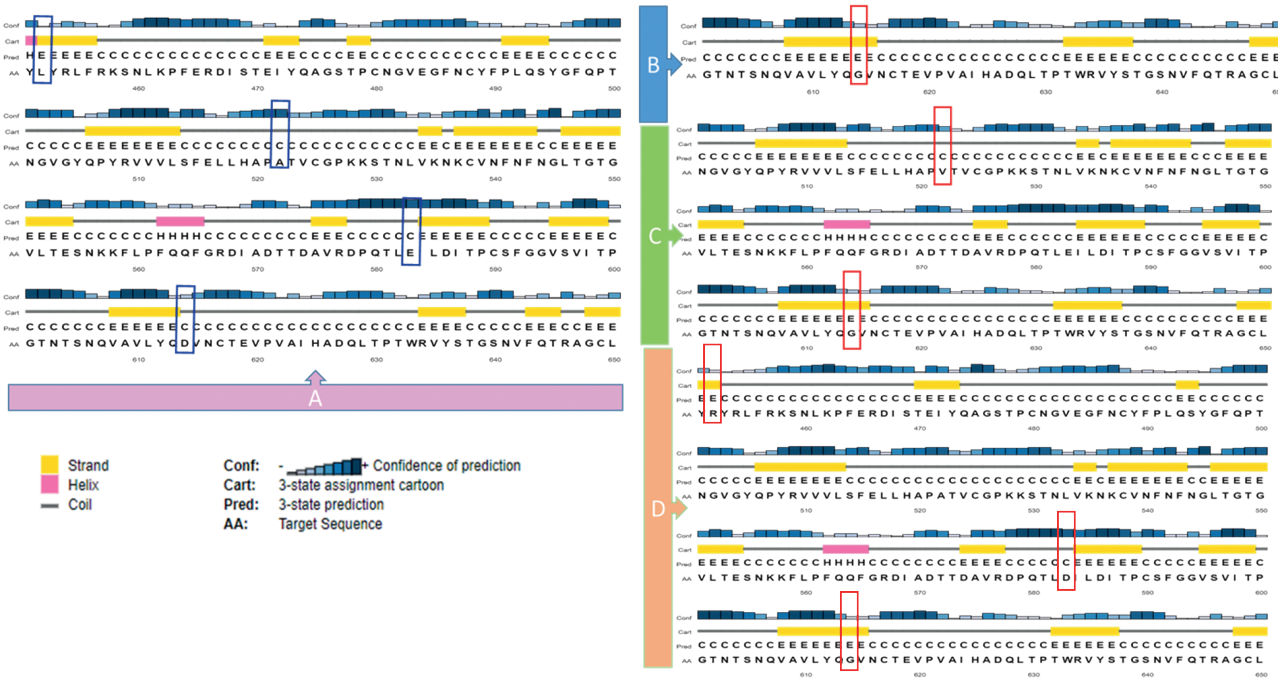

Figure 3. Prediction 2D structure of S protein sequences

Note. (A) the original residues of wild type. (B) site of D614G mutation of the strain QPI19598 in pink color. (C) site of A522V and D614G mutations of 17 strains. (D) site of L452R, E583D, and D614G mutations of the strain QRW43499.

region were: L452R mutation [lysine (L) substituted with arginine (R) in residue 452 of QRW43499. A522V mutation [alanine (A) substituted with valine (V) in residue 522 of 17 sequences. E583D mutation [glutamate (E) substituted with aspartate (D) in residue 583 of QRW43499.

Phylogenetic analyzes of the tree have shown that one genome is entirely linked to the wild form. Other sequences with various similarities in the same cladding are linked to the comparison (Figure 2).

We have shown that there is a conformational change in chains due to mutations in the prediction of two-dimensional structure. Mutations E583D and D614G have changed from the coil to the strand, but we have not seen any difference in the chains in positions L452R and A522V (Figure 3).

In global structures, like expanded random coil protein, with a poor secondary structure or molten globules, the native disorder still occurs, which have normal secondary structure elements that do not

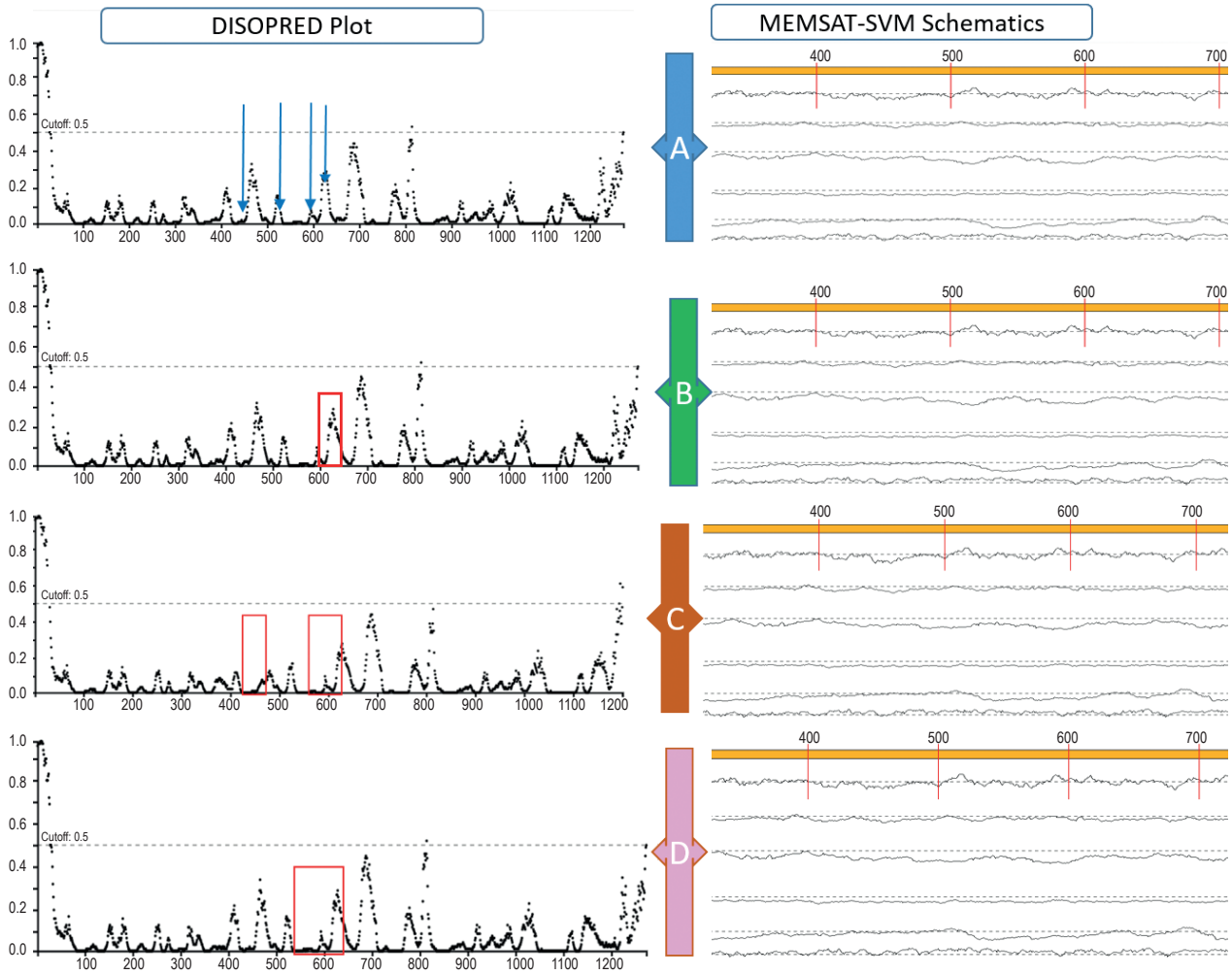

Figure 4. Analysis of Disopred (DISOPRED 3) and membrane helix prediction (MEMSAT-SVM)

Note. (A) wild type shows the original residues with blue lines in the plot and schematic. (B) D614G mutation of the strain QPI19598. (C) L452R, E583D, and D614G mutations of the strain QRW43499. (D) A522V and D614G mutations of 17 strains.

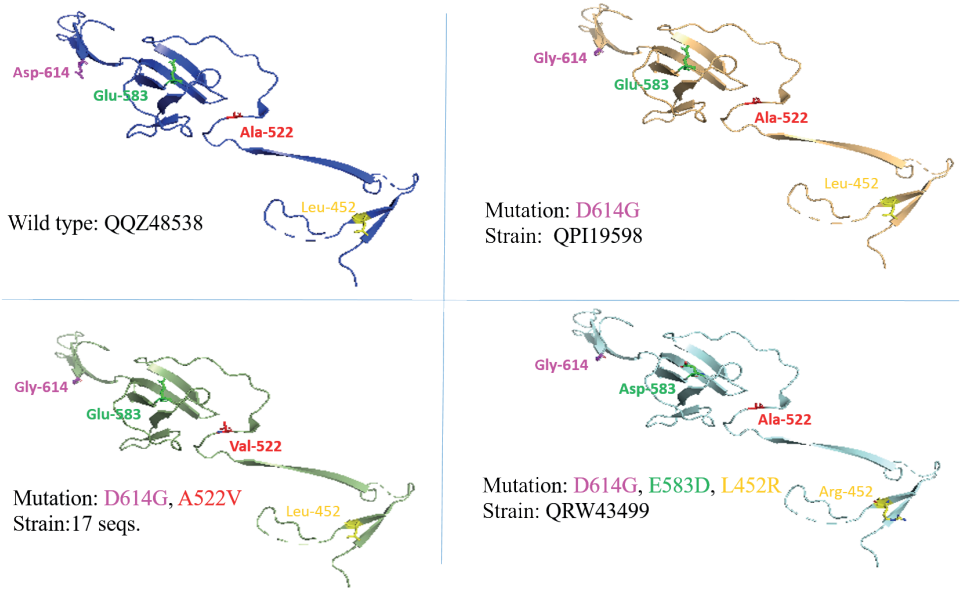

Figure 5. Cartoon 3D structure of wild type and mutant sequences

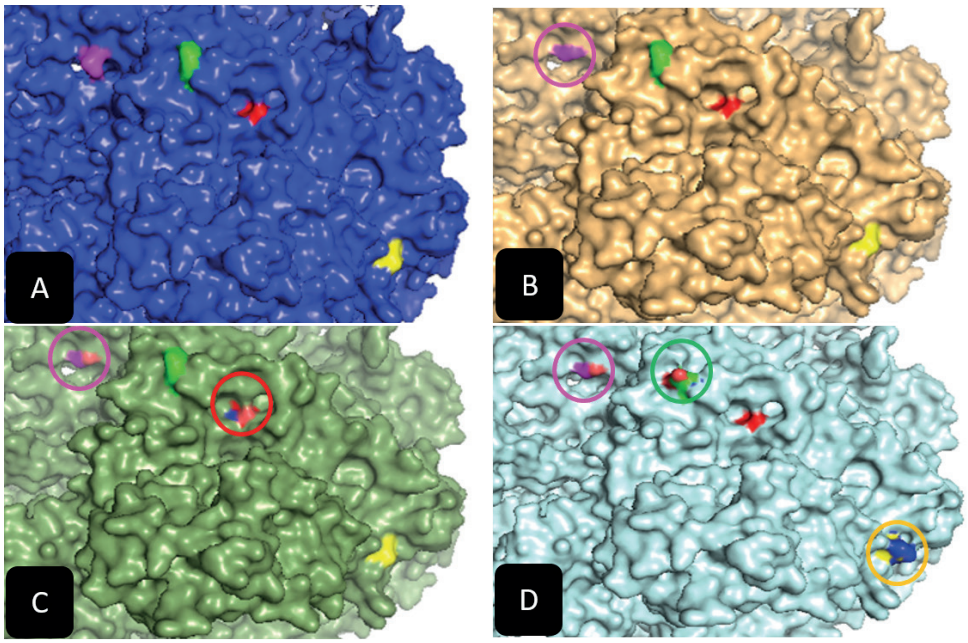

Figure 6. Surface view of the 3D structure of wild type and mutant sequences

Note. (A) wild type. (B) D614G mutation of the strain QPI19598 shows in pink color. (C) A522V and D614G mutations of 17 strains shows in red color. (D) L452R, E583D, and D614G mutations of the strain QRW43499.

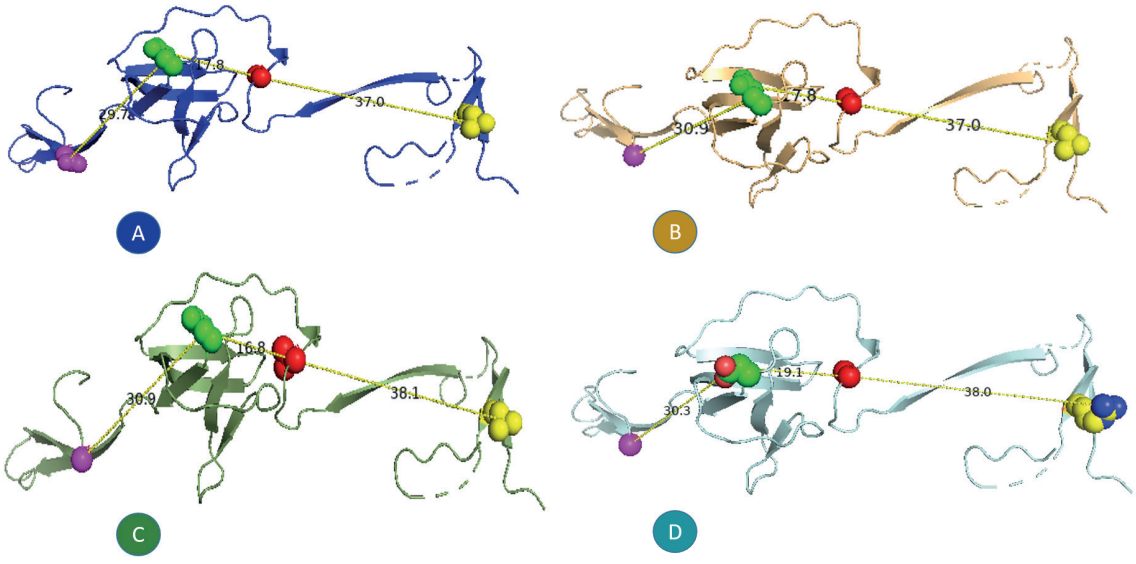

Figure 7. Measurement of distances between atoms of wild type and mutagenic patterns

Note. (A) distances between 4 residues in wild type 29.78Å, 17.8Å and 37Å. (B) distances between none mutated residues and D614G mutation of the strain QPI19598, 30.9Å, 7.8Å and 37Å respectively. (C) distances between wild residues and (A522V and D614G mutations) of 17 strains 30.9Å, 16.8Å and 38.1Å respectively. (D) distances between wild residues and (L452R, E583D, and D614G mutations) of the strain QRW43499, 30.3Å, 19.1Å and 38Å respectively.

condense into a stable globular fold. The change in the protein secondary structure can be observed by analyzing the original disorder concerning the main type and mutant strains using DISOPRED 3 server and membrane helix prediction (MEMSAT-SVM) (Figure 4).

We constructed a three-dimensional structure of the mutagenic strains obtained on the template chosen for the S protein. In the cartoon and ribbon surface models as shown in Figures 5 and 6, the photographs have shown the proportion of modifications in the protein structure and the morphological changes related to each mutation.

The findings of the study measure the distance between the wild-type atoms and the mutant strains. The current study showed that the distance between

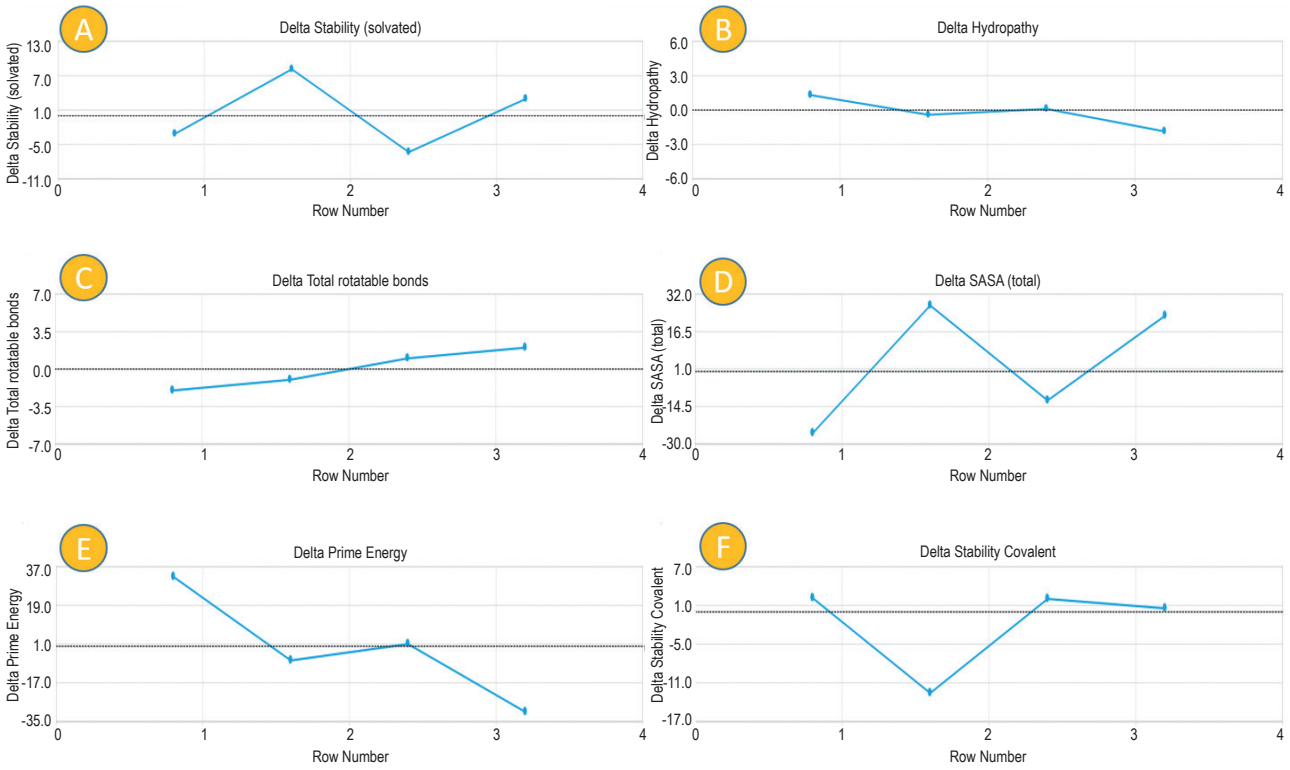

Figure 8. Energy level of 4 mutations

Note. (A) Δ Stability (solvated). (B) Δ Hydropathy. (C) Δ Total rotatable bonds. (D) Δ SASA (total). (E) Δ Prime Energy. (F) Δ Stability Covalent.

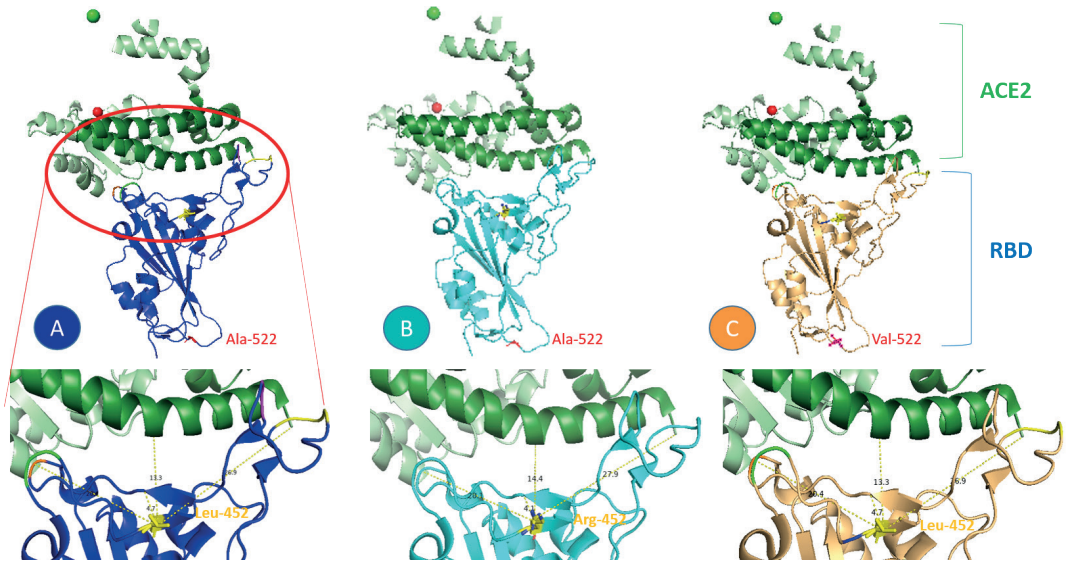

Figure 9. Molecular docking of RBD-ACE2 of wild and mutant sequences show the position of mutations in the docking interaction

Note. (A) wild type. (B) L452R mutation of the strain QRW43499. (C) A522V mutation of 17 strains.

atoms is markedly different. The spacing between residues L452R and A522V of the C3 atoms is 37 for the wild type, while the distance for the mutated type is 38 and 38.1 (Figure 7C and D) respectively. Between A522V and E583D residues, the gap between the wild and mutant strains was reduced, from 17.8 to 16.8 . The interval between C3 atoms, on the other hand, ranged from 29.7 to 30.9 between positions E583D and D614G (Figure 7). The energy calculation of atoms including hydropathy, rotatable bonds, prime

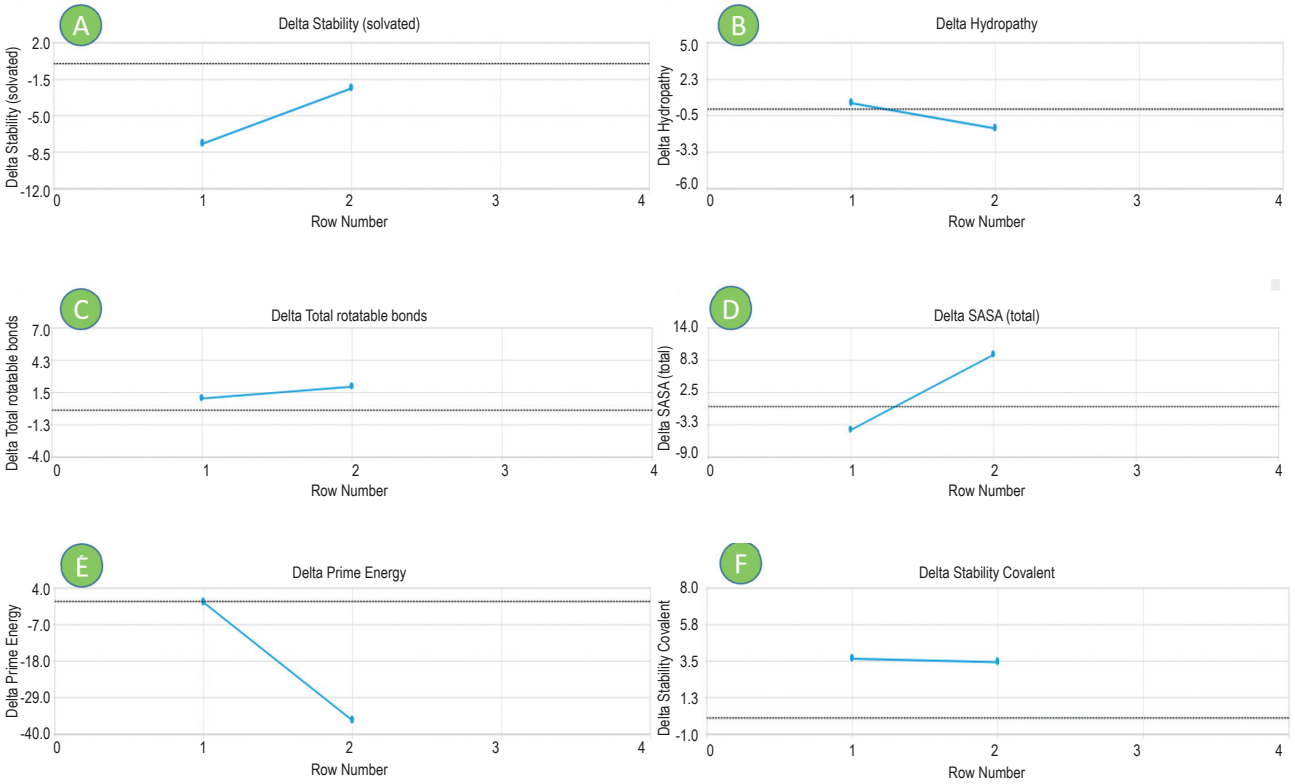

Figure 10. Energy level of 4 mutations

Note. (A) Δ Stability (solvated). (B) Δ Hydropathy. (C) Δ Total rotatable bonds. (D) Δ SASA (total). E: Δ Prime Energy. F: Δ Stability Covalent.

TABLE 1. MODIFICATION OF ENERGY EQUATIONS BETWEEN WILD AND MUTANT RESIDUES

Residue	Original	Mutate	Δ Stability (solvated) kcal/mol	Δ Hydropathy kcal/mol	Δ Total rotatable bonds kcal/mol	Δ SASA (total) kcal/mol	Δ Prime Energy kcal/mol	Δ Stability Covalent kcal/mol
A:614	Asp	Gly	-3.15	1.31	-2	-25.47	32.27	2.13
A:583	Glu	Asp	8.12	-0.41	-1	27.30	-6.60	-12.59
A:522	Ala	Val	-6.34	0.10	1	-11.97	1.03	2.01
A:452	Leu	Arg	2.95	-1.86	2	23.08	-30.55	0.54

TABLE 2. MODIFICATION OF ENERGY EQUATIONS BETWEEN WILD AND MUTANT RESIDUES

Residue	Original	Mutate	Δ Stability (solvated) kcal/mol	Δ Hydropathy kcal/mol	Δ Total rotatable bonds kcal/mol	Δ SASA (total) kcal/mol	Δ Prime Energy kcal/mol	Δ Stability Covalent kcal/mol
A:522	Ala	Val	-7.68	0.45	1	-4.14	-0.31	3.65
A:452	Leu	Arg	-2.37	-1.46	2	9.23	-35.87	3.44

energy, stability solvate, and covalent bonds resulting from mutations was shown in table (1). The mutations have led to the protein stability by reading the data, especially for the E583D and D614G mutations (Figure 8).

The receptor-binding domain (RBD), which is part of the S1 subunit, responsible for the docking of S protein to the ACE2 receptor on the host cell membrane. PDB (6M0J) was selected to detect mutation effects and build the three-dimensional structure of new mutations. The RBD region contains residues in the range of (333-526). There are only two detected mutations found in it (Arg-452 and Val-522). RBD interface fusion residues include sites (473-508), while ACE2 molecular docking residues include sites (21-100). Since the observed mutations do not occur inside the fusion site, but rather through the construction of the crystal structure, it became apparent that mutation Arg-452 has an impact on the fusion site. We noticed a change in the distance between the carbon atom no. 3 and the fusion sites for the wild type (26.9 , 13.3 , 4.7 , and 20.4), while for the mutated type it was (27.9Å, 14.4Å, 4.1 , and 20.1Å). In this study, we did not observe a change concerning mutation Val-522 in the coalescence region because it is relatively distant (Figure 9). The energy calculation of atoms including hydropathy, rotatable bonds, prime energy, stability solvate, and covalent bonds resulting from 2 mutations was shown in table (2). Since the energy of a solvated bond is greater than the energy of a covalent bond, the mutations L452R and A522V result in stability proteins. This finding may affect the total energy of the RBD-ACE2 docking fusion residues (Figure 10).

Discussion

Despite the development of vaccines for the emerging coronavirus, scientists are still trying to figure out how the virus interacts with the host cell. Researchers are also working to restrict the virus by detecting mutations and thereby preventing it from entering the cell [33, 36].

Several genomic regions of increased genetic variation in SARS-CoV-2 isolates were discovered in recent studies of fine-scale sequence variation [20, 23]. We discovered four apparent mutations by studying the amino acid sequence pattern of the selected strains. The most common mutation (D614G) in the second wave of the epidemic in Brazil and the United Kingdom was detected in 19 sequences [15]. In many of the places where it has been detected, the mutant virus with glycine at the residue (G614) has shown to quickly dominate [31, 37]. This finding indicates that the G614 virus may have a propagation advantage over the D614 virus, but we can't rule out the possibility that non-stochastic sampling of virus sequences and spontaneous founder effects contribute to its current dominance [11, 22]. The D614G mutation is thought to facilitate an open configuration of the S protein that is more conducive to ACE2 association [27, 34].

The wild form was followed by one strain. Three mutations were also discovered (L452R, A522V, and E583D). Three forms of mutations were found in the strains (QRW43499). By predicting the two-dimensional structure of mutated strains, it became clear to us that there is a change in the shape of the chain from the coil to strand for the two mutations (E583D and D614G). This is yet another example of how modifying the protein's two-dimensional structure affects its three- dimensional form. This confirms that using the Disopred server, the mutation frequency for the wild type has increased, particularly for the D614G mutant. An amino acid modification (D614G) outside the RBD was shown to be more contagious in a previous study, but no evidence of being immune to neutralizing antibodies was found. The increasing domination of D614G, on the other hand, needs special consideration [2, 29].

After constructing the mutants' crystal structures and comparing them to the wild form, we discovered that there is a significant difference, especially in the surface view of residue mutation L452R. The conformational change in the distance between the atoms confirms this. On the other hand, variations in energy measurements that were often directed toward protein stability were observed. The solvate energies of D614G and A522V are lesser than those of E583D and L452R. In contrast to the rest of the mutations, the energy of the covalent bonds was lower in the position E583D.

We conducted that the L452R mutation is nearest to the fusion region and has an effect on the protein's structure, while the A522V mutation has little effect on the overall shape due to its distance from the fusion region (473-508). What confirms our perception is the change of the distances between the atoms for the mutated from the wild type. As compared to the energy of covalent bonds, the solvated energy of the two mutations was stronger. When we equate the mutational energy of protein S to the mutagenic energy of RBD-ACE2 molecular docking, we find an important difference. For example, the solvate energy for the L452R mutation in the S protein was (2.95 kcal/mol), while the same mutation in RBD-ACE2 had lower energy (-2.37 kcal/mol). The rotatable energy between S protein mutations and RBD-ACE2 docking was revealed to be unchanged in the current study. Furthermore, the study recorded important variations in the various energies of mutations under study between S protein and RBD-ACE2 molecular docking.

S protein conformational changes that result in membrane fusion include not only receptor binding but also adequate protease activation. It's also helpful to know the rate and pace of mutations because they play a key role in the virus eluding the host immune system and increasing drug resistance [10]. We speculated that since human ACE2 hasn't adapted to

accept the SARS-CoV-2 S enzyme, mutations that increase affinity could be discovered. Without a doubt, mutations in the S protein play the most important role in modifying the virus's pattern of host-cell attachment and interaction. It's also crucial to know the rate and pace of mutations because they play a key role in the virus eluding the host immune system and gaining drug resistance [31].

According to one review, the furin-cleavage site tends to confer a fitness benefit that has yet to be determined. The D614G S-protein mutation that tends to facilitate SARS-CoV-2 transmission in humans also improves functional S-protein integration into SARS-CoV-2 VLP and retroviral PV, increasing PV infectivity [38]. To assess the effect of this transition on the existence and magnitude of COVID-19, further research will be needed.

Our findings suggest that stabilizing mutations will keep S protein stable enough to perform its function and also improving SARS-CoV-2 resistance. Via calculating energy variations, we conducted that the viral mutants are substitutions with minimum and maximum folding.

Conclusions

We investigated 20 sequences of SARS-CoV-2 S protein missense mutation isolates in Iraq using computational saturation mutagenesis. We found 19 strains with the common mutation (D614G) that can stabilize the whole SARS-Cov-2 S protein. Furthermore, we conducted that the majority of mutation sites would improve the S protein's stability. One strain, published on February 25, 2021, included three mutations, which is a dangerous sign that the number of mutations in the S protein may increase. We also revealed that neighboring residues L452R and A522V have distinct effects on RBD-ACE2 binding. The effect of the mutation site on the S protein and the location of docking fusion differs due to differences in the measured energy ratios of atoms, which is essential for this protein-protein interaction.

Acknowledgments

The authors express their gratitude to the medical colleges of Nineveh and Mosul for recording their work.

References

1. Bestle D., Heindl M.R., Limburg H., Pilgram O., Moulton H., Stein D.A., Hardes K., Eickmann M., Dolnik O., Rohde C., Klenk H.-D., Garten W., Steinmetzer T., Böttcher-Friebertshäuser E. TMPRSS2 and furin are both essential for proteolytic activation and spread of SARS-CoV-2 in human airway epithelial cells and provide promising drug targets. *Life Sci. Alliance, 2020, Vol. 3, e202000786.* doi: 10.26508/lsa.202000786.

2. Bosch B.J., van der Zee R., de Haan C.A., Rottier P.J. The coronavirus spike protein is a class I virus fusion protein: structural and functional characterization of the fusion core complex. *J. Virol., 2003, Vol. 77, no. 16, pp. 8801-8811.*

3. Calcagnile M., Forgez P., Lannelli A., Bucci C., Alifano M., Alifano P. Molecular docking simulation reveals ACE2 polymorphisms that may increase the affinity of ACE2 with the SARS-CoV-2 Spike protein. *Biochimie, 2021, Vol. 180, pp. 143-148.*

4. Chan K., Dorosky D., Shamra P., Abbasi S., Dye J., Kranz D., Herbert A.S. Procko E. Engineering human ACE2 to optimize binding to the spike protein of SARS coronavirus 2. *Science, 2020, Vol. 369, no. 6508, pp. 1261-1265.*

5. Dawood A. Glycosylation, ligand binding sites and antigenic variations between membrane glycoprotein of COVID-19 and related coronaviruses. *Vacunas, 2021, Vol. 22, no. 1, pp. 1-9.*

6. Dawood A. Identification of CTL and B-cell epitopes in the Nucleocapsid Phosphoprotein of COVID-19 using Immunoinformatics. *Microbiol. J., 2021, Vol. 83, no. 1, pp. 78-86.*

7. Dawood A. Mutated COVID-19, May Foretells Mankind in a Great Risk in The Future. *New Microbes New Infect., 2020, Vol. 35, 100673.* doi: 10.1016/j.nmni.2020.100673.

8. Dawood A., Altobje M. Inhibition of N-linked Glycosylation by Tunicamycin May Contribute to The Treatment of SARS-CoV-2. *Microbiol. Path.*, 2020*, Vol. 149, 104586.* doi: 10.1016/j.micpath.2020.104586.

9. Dawood A., Altobje M., Alnori H. Compatibility of the ligand binding sites in the spike glycoprotein of COVID-19 with those in the aminopeptidase and the caveolins 1, 2 proteins. *Res. J. Pharm. Tech., 2021, Vol. 14, no. 9, pp. 4760-4766.* Wu F., Zhao S., Yu B., Chen Y.M, Wang W., Song Z.G., Hu Y., Tao Z.-W., Tian J.-H., Pei Y.-Y., Yuan M.-L., Zhang Y.-L., Dai F.-H., Liu Y., Wang Q.-M., Zheng J.-J., Xu L., Holmes E.C., Zhang Y.-Z. A new coronavirus associated with human respiratory disease in China. *Nature, 2020, Vol. 579, pp. 265-269.*

10. Dawood A., Altobje M., Alrassam Z. Molecular Docking of SARS-CoV-2 nucleocapsid protein with angiotensin-converting enzyme II. *Mikrobio Zhu., 2021, Vol. 83, no. 2, pp. 82-92.*

11. Dieterle M.E., Haslwanter D., Bortz III R.H., Wirchnianski A.S., Lasso G., Vergnolle O., Abbasi S.A., Fels J.M., Laudermilch E., Florez C., Mengotto A., Kimmel D., Malonis R.J., Georgiev G., Quiroz J., Barnhill J., Pirofski L.-A., Daily J.P., Dye J.M., Lai J.R., Herbert A.S., Chandran K., Jangra R.K. A replication-competent vesicular stomatitis virus for studies of SARS-CoV-2 spike-mediated cell entry and its inhibition. *Cell Host Microbe, 2020, Vol. 28, no. 3, pp. 486-496.e6.*

12. Duan L., Zheng Q., Zhang H., Nlu Y., Wang H. The SARS-CoV-2 spike glycoprotein biosynthesis, structure, function, and antigenicity: implications for the design of spike-based vaccine immunogens. *Front. Immunol. 2020, Vol. 11, 576622.* doi: 10.3389/fimmu.2020.576622.

13. Durmaz B., Abdulmajed O., Durmaz R. Mutations observed in the SARS-CoV-2 spike glycoprotein and their effects in the interaction of virus with ACE-2 receptor. *Medeni Med. J., 2020, Vol. 35, no. 3, pp. 253-260.*

14. Hoffmann M., Kleine-Weber H., Schroeder S., Kruger N., Herrler T., Erichsen S., Schiergens T.S., Herrler G., Wu N.-H., Nitsche A., Müller M.A. Drosten C., Pöhlmann S. SARS- CoV-2 cell entry depends on ACE2 and TMPRSS2 and is blocked by a clinically proven protease inhibitor. *Cell, 2020, Vol. 181, no. 2, pp. 271-280.e8.*

15. Iwanaga N., Cooper L., Rong L., Beddingfield B., Crabtree J., Tripp R.A., Qin X., Kolls J.K. Novel ACE2-IgG1 fusions with increased activity against SARS-CoV-2. *bioRxiv, 2020.* doi: 10.1101/2020.06.15.152157.

16. Lan J., Ge J., Shan S., Zhou H., Fan S., Zhang Q., Shi X., Wang Q., Zhang L., Wang X. Structure of the SARS-CoV-2 spike receptor-binding domain bound to the ACE2 receptor. *Nature, 2020, Vol. 581, no. 7807, pp. 215-231.*

17. Lan J., Ge J., Yu J., Shan S., Zhou H., Fan S., Zhang Q., Shi X., Wang Q., Zhang L., Wang X. Structure of the SARS-CoV-2 spike receptor-binding domain bound to the ACE2 receptor. *Nature, 2020, Vol. 581, no. 7807, pp. 215-220.*

18. Lei C., Qian K., Li T., Zhang S., Fu W., Ding M., Hu S. Neutralization of SARSCoV-2 spike pseudotyped virus by recombinant ACE2-Ig. *Nat. Commun., 2020, Vol. 11, no. 1, 2070.* doi: 10.1038/s41467-020-16048-4.

19. Letko M., Marzi A., Munster V. Functional assessment of cell entry and receptor usage for SARS-CoV-2 and other lineage B betacoronaviruses. *Nat. Microbiol., 2020, Vol. 5, pp. 562-569.*

20. Liang Y., Wang M.-L., Chien C.-S., Yarmishyn A.A., Yang Y.-P., Lai W.-Y., LuoY .-H., Lin Y.-T., Chen Y.-J., Chang P.-C., Chiou S.-H. Highlight of immune pathogenic response and hematopathologic effect in SARS-CoV, MERS-CoV, and SARS-Cov-2 infection. *Front. Immunol., 2020, Vol. 11, 1022.* doi: 10.3389/fimmu.2020.01022.

21. Li Q., Wu J., Nie J., Zhang L., Hao H., Liu S., Zhao C., Zhang Q., Liu H., Nie L., Qin H., Wang M., Lu Q., Li X., Sun Q., Liu J., Zhang L., Li X., Huang W., Wang Y. The impact of mutations in SARS-CoV-2 spike on viral infectivity and antigenicity. *Cell, 2020, Vol. 182, no. 5, pp. 1248-1294.*

22. Malik Y.A. Properties of Coronavirus and SARS-CoV-2. *Malays. J. Pathol., 2020, Vol. 42, no. 1, pp. 3-11.*

23. Monteil V., Kwon H., Prado P., Hagelkruys A., Wimmer R.A., Stahl M., Leopoldi A., Garreta E., Hurtado Del Pozo C., Prosper F., Romero J.P , Wirnsberger G., Zhang H., Slutsky A.S., Conder R., Montserrat N., Mirazimi A., Penninger J.M. Inhibition of SARS-CoV-2 infections in engineered human tissues using clinical-grade soluble human ACE2. *Cell, 2020, Vol. 181, no. 4, pp. 905-913.e7.*

24. Othman H., Bouslama Z., Brandenburg J.T., Rocha J., Hamdi Y., Ghedira K., Srairi-Abid N., Hazelhurst S. Interaction of the spike protein RBD from SARS-CoV-2 with ACE2: Similarity with SARS-CoV, hot- spot analysis and effect of the receptor polymorphism. *Biochem. Biophys. Res. Comm., 2020, Vol. 527, no. 3, pp. 702-710.*

25. Othman H., Bouslama Z., Brandenburg J.T., Rocha J., Hamdi Y., Ghedira K., Srairi-Abid N., Hazelhurst S. In silico study of the spike protein from SARS-CoV-2 interaction with ACE2: similarity with SARS- CoV, hot-spot analysis and effect of the receptor polymorphism. *BioRxiv, 2020,* 339781420. doi: 10.1101/2020.03.04.976027.

26. Ou X., Liu Y., Lei X., Li P., Mi D., Ren L., Guo L., Guo R., Chen T., Hu J., Xiang Z., Mu Z., Chen X., Chen J., Hu K., Jin Q., Wang J., Qian Z. Characterization of spike glycoprotein of SARS-CoV-2 on virus entry and its immune cross-reactivity with SARS-CoV. *Nature Comm., 2020, Vol. 11, no. 1, 1620.* doi: 10.1038/s41467-020-15562-9.

27. Schmidt F., Weisblum Y., Muecksch F., Hoffmann H.-H., Michailidis E., Lorenzi J.C., Mendoza P., Rutkowska M., Bednarski E., Gaebler C., Agudelo M., Cho A., Wang Z., Gazumyan A., Cipolla M., Caskey M., Robbiani D.F., Nussenzweig M.C., Rice C.M., Hatziioannou T., Bieniasz P.D. Measuring SARS-CoV-2 neutralizing antibody activity using pseudotyped and chimeric viruses. *J. Exp. Med., 2020, Vol. 217, no. 11, e20201181.* doi: 10.1084/jem.20201181.

28. Shang J., Ye G., Shi K., Wan Y., Luo C., Aihara H., Geng Q., Auerbach A., Li F. Structural basis of receptor ecognition by SARS-CoV-2. *Nature, 2020, Vol. 581, no. 7807, pp. 221-239.*

29. Tai W., He L., Zhang X., Pu J., Voronin D., Jiang S., Zhou Y., Du L. Characterization of the receptor-binding domain (RBD) of 2019 novel coronavirus: implication for development of RBD protein as a viral attachment inhibitor and vaccine. *Cell. Mole. Immunol., 2020, Vol. 17, no. 6, pp. 613-620.*

30. Tang T., Bidon M., Jaimes J.A., Whittaker G.R., Daniel S. Coronavirus membrane fusion mechanism offers apotential target for antiviral development. *Antiviral Res., 2020, Vol. 178, 104792.* doi: 10.1016/j.antiviral. 2020.104792.

31. Teng S., Sobitan A., Rhoades R., Liu D., Tang Q. Systemic effects of missense mutations on SARS-CoV-2 spike glycoprotein stability and receptor-binding affinity. *Brief Bioinf., 2021, Vol. 22, no. 2, pp. 1239-1253.*

32. Ujike M., Huang C., Shirato K., Makino S., Taguchi F. The contribution of the cytoplasmic retrieval signal of severe acute respiratory syndrome coronavirus to intracellular accumulation of S proteins and incorporation of S protein into viruslike particles. *J. Gen. Virol., 2016, Vol. 97, no. 8, pp. 1853-1864.*

33. Wang Q., Zhang Y., Wu L., Niu S., Song C., Zhang Z., Lu G., Qiao C., Hu Y., Yuen K.-Y. , Wang Q., Zhou H., Yan J., Qi J. Structural and Functional Basis of SARS-CoV-2 Entry by Using Human ACE2. *Cell, 2020, Vol. 181, no. 4, pp. 894-904.e9.*

34. Wrapp D., Wang N., Corbett K.S., Goldsmith J.A., Hsieh C.L., Abiona O., Graham B.S. , McLellan J.S. Cryo-EM structure of the 2019-nCoV spike in the prefusion conformation. *Science, 2020, Vol. 367, no. 6483, pp. 1260-1263.*

35. Wu F., Zhao S., Yu B., Chen Y.M., Wang W., Song Z.G, A new coronavirus associated with human respiratory disease in China. *Nature, 2020, Vol. 579, pp. 265-269.*

36. Yan R., Zhang Y., Li Y., Xia L., Guo Y., Zhou Q. Structural basis for the recognition of SARS-CoV-2 by full-length human ACE2. *Science, 2020, Vol. 367, no. 6485, pp. 1444-1448.*
37. Zhang G., Pomplun S., Loftis A.R., Loas A., Pentelute B. Thefirst-in-class peptide binder to the SARS-CoV-2 spike protein. *bioRxiv. 2020.* doi: 10.1101/2020.03.19.999318.
38. Zhang L., Jackson C., Mou H., Ojha A., Quinlan B., Ranarajan E., Izard T., Farzan M., Choe H. SARS-CoV-2 spike- protein D614G mutation increases virion spike density and infectivity. *Nature Comm*., 2020, Vol. 11, 6013. doi: 10.1038/s41467-020-19808-4.

Авторы:

Али А. Давуд *– к.микробиол.н., лектор, кафедра анатомии Медицинского колледжа Мосульского университета, г. Мосул, Ирак*

Бассам Исмаил Ясим *– Ниневийский университет, г. Мосул, Ирак*

Омар Рияд-аль-Джалили *– Мосульсий университет, г. Мосул, Ирак*

Authors:

Ali A. Dawood, *PhD (Microbiology), Lector, Department of Anatomy, College of Medicine, University of Mosul, Mosul, Iraq*

Bassam Ismael Jasim, *Ninevah University, Mosul, Iraq*

Omar Riadh Al-Jalily, *University of Mosul, Mosul, Iraq*

Поступила 17.12.2021
Отправлена на доработку 07.01.2022
Принята к печати 07.03.2022

Received 17.12.2021
Revision received 07.01.2022
Accepted 07.03.2022